Ediacaran reorganization of the marine phosphorus cycle

Thomas A. Laakso[a,1], Erik A. Sperling[b], David T. Johnston[a], and Andrew H. Knoll[c,1]

[a]Department of Earth and Planetary Sciences, Harvard University, Cambridge, MA 20138; [b]Department of Geological Sciences, Stanford University, Stanford, CA 94305; and [c]Department of Organismic and Evolutionary Biology, Harvard University, Cambridge, MA 20138

Contributed by Andrew H. Knoll, March 25, 2020 (sent for review September 26, 2019; reviewed by Kurt O. Konhauser and Lee R. Kump)

The Ediacaran Period (635 to 541 Ma) marks the global transition to a more productive biosphere, evidenced by increased availability of food and oxidants, the appearance of macroscopic animals, significant populations of eukaryotic phytoplankton, and the onset of massive phosphorite deposition. We propose this entire suite of changes results from an increase in the size of the deep-water marine phosphorus reservoir, associated with rising sulfate concentrations and increased remineralization of organic P by sulfate-reducing bacteria. Simple mass balance calculations, constrained by modern anoxic basins, suggest that deep-water phosphate concentrations may have increased by an order of magnitude without any increase in the rate of P input from the continents. Strikingly, despite a major shift in phosphorite deposition, a new compilation of the phosphorus content of Neoproterozoic and early Paleozoic shows little secular change in median values, supporting the view that changes in remineralization and not erosional P fluxes were the principal drivers of observed shifts in phosphorite accumulation. The trigger for these changes may have been transient Neoproterozoic weathering events whose biogeochemical consequences were sustained by a set of positive feedbacks, mediated by the oxygen and sulfur cycles, that led to permanent state change in biogeochemical cycling, primary production, and biological diversity by the end of the Ediacaran Period.

Ediacaran | biosphere | sulfate | phopshorus | phosphorite

For more than 3 billion years, Earth's surface was characterized by low primary production, limited atmospheric oxygen, and a predominantly microbial biota (1–3). The transition to a more productive biosphere, with relatively high partial pressure of oxygen (pO_2), macroscopic animals, and eukaryotic phytoplankton, began, or at least accelerated, during the Ediacaran Period (635 to 541 Ma), as evidenced by both fossils and geochemical signatures. Macroscopic animals occur in rocks as old as 575 Ma (4, 5), and bilaterian body fossils appear by 15 million years later [refs. 6 and 7; note that earlier Ediacaran trace fossils have been claimed (8)]. Increased oxygen and food supply have both been advanced as environmental prerequisites for animal diversification (9–12), a view that gains support from biomarker (13, 14), microfossil (15), and molecular clock evidence (16) for the Ediacaran emergence of eukaryotic phytoplankton after more than 3 billion years of prokaryotic dominance. As eukaryotic phytoplankton tend to displace cyanobacteria when nutrients are plentiful, this provides prima facie evidence for increasing primary production, with its consequences for both oxygen availability and food supply (17, 18). Geochemical data provide further, independent evidence for Ediacaran redox change (19).

Tectonics has long been proposed as a principal driver of Ediacaran Earth system transition, with specific attention paid to Pan-African orogenesis as the source of increased phosphorus fluxes into the world's oceans (20). More recently, Williams et al. (21) have argued that increased carbon fluxes from continental arc volcanoes fueled expanding primary production, but unless productivity was earlier limited by carbon availability this also requires an increased nutrient supply. The termination of Cryogenian glaciations may also have introduced a large, albeit transient, pulse of phosphorus into the oceans of the very earliest Ediacaran Period (22). Phosphorus-based hypotheses for Ediacaran biosphere transition are attractive, but those articulated to date suffer from problems of transience and, possibly, magnitude. Increased weathering and erosion might, under favorable conditions, transiently increase P flux to the oceans by a factor of 2 or so, but we argue below that the sedimentary record of phosphorites (Fig. 1) likely indicates order-of-magnitude changes in P supply to phosphogenic environments. Increased erosional fluxes are also inherently limited in time; once the tectonic events under consideration end, the system will revert back to its antecedent state. As Kump (23) noted, "Any viable explanation for stepwise oxygen evolution must involve a fundamental change in the way the Earth system operates; perturbations, even massive organic carbon burial events, bolide impacts, or flood basalt eruptions, in themselves cannot effect permanent change in Earth's surface environment."

Here we argue the case for tectonics and nutrient supply from a different perspective, motivated by the abrupt appearance of massive phosphorite deposits beginning in the Ediacaran Period. Specifically, we argue that increased regeneration and upwelling of P, the consequence of sulfur input associated with Pan-African orogenesis and/or postglacial weathering, increased the sulfate and oxygen inventories of the oceans, thereby setting in motion positive feedbacks that permanently altered the Earth system. On modern Earth, nutrients regenerated at depth in oceanic basins and subsequently upwelled outpace the delivery of P from continents by orders of magnitude (24), providing a

Significance

The evolution of macroscopic animals in the latest Proterozoic Eon is associated with many changes in the geochemical environment, but the sequence of cause and effect remains a topic of intense research and debate. In this study, we use two apparently paradoxical observations—that massively phosphorus-rich rocks first appear at this time, and that the median P content of rocks does not change—to argue for a change in internal marine P cycling associated with rising sulfate levels. We argue that this change was self-sustaining, setting in motion a cascade of biogeochemical transformations that led to conditions favorable for major ecological and evolutionary change.

Author contributions: T.A.L., D.T.J., and A.H.K. designed research; T.A.L., E.A.S., D.T.J., and A.H.K. performed research; T.A.L., E.A.S., D.T.J., and A.H.K. analyzed data; and T.A.L., E.A.S., D.T.J., and A.H.K. wrote the paper.

Reviewers: K.O.K., University of Alberta; and L.R.K., Pennsylvania State University.

The authors declare no competing interest.

[1]To whom correspondence may be addressed. Email: laakso@fas.harvard.edu or aknoll@oeb.harvard.edu.

This article contains supporting information online at https://www.pnas.org/lookup/suppl/doi:10.1073/pnas.1916738117/-/DCSupplemental.

First published May 18, 2020.

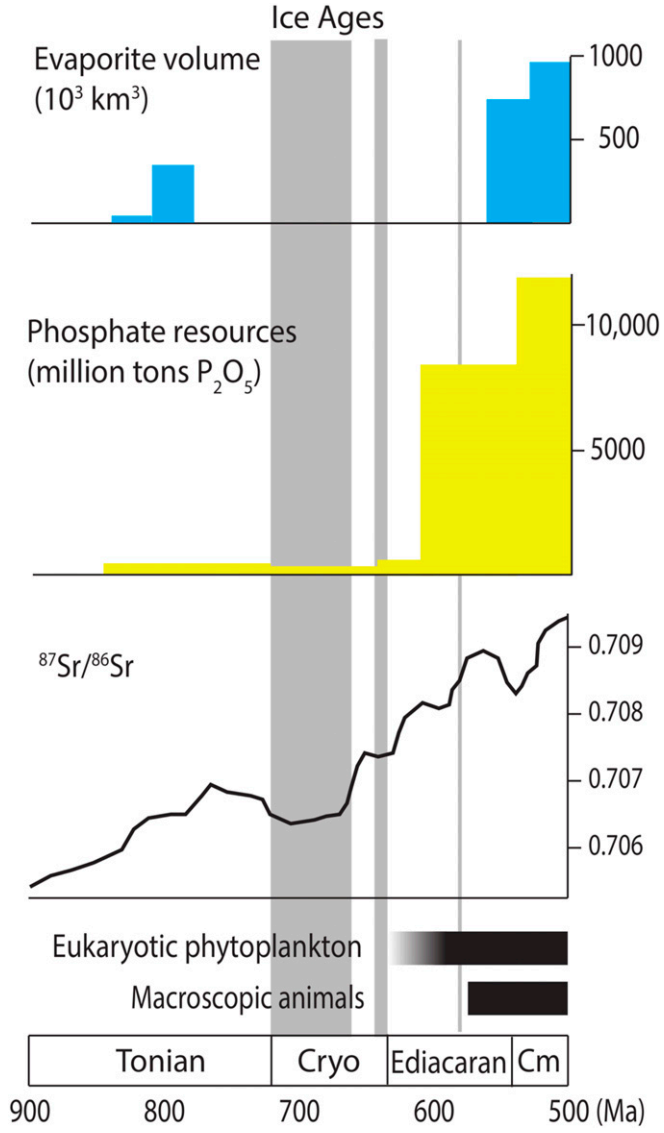

Fig. 1. Neoproterozoic to Cambrian secular variations in biogeochemical and paleontological records. These include sedimentary phosphorite resources, evaporite deposits, and Sr isotopic abundances in limestones, and within this context the rise of eukaryotic phytoplankton to ecological prominence and the appearance of macroscopic animals. Sources of data: evaporites (35), phosphorites (27, 74), strontium isotopes (43), phytoplankton (14), animal fossils (4). Note that resource estimation for pre-Ediacaran phosphorites can be challenging as most deposits are small and so attract limited industry interest.

massive biogeochemical lever on primary production and a sustainable positive feedback on the scale of the carbon and nutrient turnover in the ocean.

Geological Observations: Fossils, Phosphorite, and Sulfate

A first-order feature of the stratigraphic record, and one that has underpinned previous hypotheses about late Proterozoic biospheric change, is the seemingly abrupt Ediacaran appearance of giant phosphorite deposits (Fig. 1). Phosphorites, sedimentary rocks with unusually high phosphorus content (>18 wt % P_2O_5; ref. 25), have been documented throughout the Proterozoic Eon (26–28), but in general phosphate-rich rocks are a minor feature of the sedimentary record until about 600 Ma (27). The oldest major phosphorites in shallow marine successions postdate Marinoan cap carbonates but, where known, predate the *ca*. 580-million-yr-old (Ma) Gaskiers glaciation. Zircon geochronology from an ash bed directly overlying ore-grade phosphorite in the Ediacaran Doushantuo Formation places a minimum constraint of 609 ± 5 Ma on the timing of regional phosphogenesis (29). A second pulse of phosphorite deposition began later in the Ediacaran Period (*ca*. 560 to 550 Ma; ref. 30), with volumetrically large phosphorite deposits continuing into the Cambrian Period and beyond.

When averaged over million-year time scales, phosphorites remove <0.01% of the riverine P input flux (24, 31). Under a steady-state scenario, therefore, net P removal from the ocean should be changed little by increasing phosphorite accumulation (discussed below). Nevertheless, the onset and persistence of a new mode of phosphorus deposition indicates that, in parallel with its biological transformations, the Ediacaran Period witnessed a state change in the global phosphorus cycle. Phosphorus plays a unique role in marine biogeochemistry, ecology and, hence, evolution because of its status as a globally limiting nutrient (32). Indeed, the global shift in phosphorite deposition correlates with other notable transitions in the biogeochemical and paleontological records (Fig. 1). As noted above, an abundance of green algal steranes is first observed locally in rocks associated with Marinoan deglaciation and occurs globally by the mid-Ediacaran Period (13, 14). Macroscopic animals and/or other large, complex eukaryotes also first appear during this interval, with anatomically simple organisms that probably fed by osmotrophy and phagocytosis appearing no later than 575 Ma. Unambiguous bilaterians, with likely higher metabolic demands, are present by ~560 Ma (6, 7). Trace metal enrichments (19) are consistent with a permanent, if perhaps limited (33), increase in oxygen concentration as early as 580 Ma, while sulfur isotope systematics (34) and the deposition of large sulfate evaporites (35) indicate increasing levels of seawater sulfate through this same interval.

It is important to ask whether Ediacaran increases in phosphorite and evaporite inventories might primarily reflect preservation rather than deposition. It has long been understood that sediment volume decreases through progressively older intervals, with a particularly prominent decline near the Proterozoic–Phanerozoic boundary (36, 37). A recent compilation of carbonates through time, however, emphasizes that although globally aggregated stratigraphic thickness per million years is much higher for Ediacaran and Cambrian carbonates than for earlier examples, the total thickness of carbonates documented for pre-Ediacaran Proterozoic time is substantially larger than that of the Ediacaran and Cambrian Periods (38). Moreover, a high proportion of pre-Ediacaran carbonates represent peritidal environments, where one might expect evaporites to precipitate. In fact, evaporites and phosphorites are not absent from the Proterozoic record; they are simply much smaller. Thus, while we do not discount the influence of preferential preservation on phosphorite and evaporite stratigraphy, we believe that the strong Ediacaran increase in these lithologies reflects, in no small part, shifting ecosystems and ocean chemistry.

In the modern ocean, phosphogenesis is the product of a phosphorus cycle largely under biological control. As a limiting nutrient, P is held to exceedingly low concentrations in surface waters. Some of the biological materials formed in the photic zone sink to deeper water masses, where the P they contain is largely recovered through remineralization. In fact, the flux of remineralized P to the surface ocean through upwelling is ~60 times greater than that sourced from rivers (24). Sediment phosphogenesis occurs primarily where these nutrient-rich upwelling water masses intersect shallow-water seafloors with high-energy "scouring" conditions and/or low rates of terrigenous sediment input (25, 39). High rates of primary production follow from the delivery of nutrient-rich deep waters to the photic zone,

increasing the flux of organic P to sediments, where it may become bound into authigenic carbonate fluorapatite. Apatite particles are concentrated by winnowing or sorting during transport, though highly productive areas with low background sedimentation may achieve phosphorus contents of >10 wt % without postdepositional concentration (39). Sedimentology and petrography suggest similar first-order controls on ancient phosphogenesis (27). The intersection of the required conditions, particularly over large spatial scales and for extended periods of time, has likely varied over Earth's history, resulting in the episodic nature of post-Ediacaran phosphogenesis. However, there is little reason to expect upwelling of water over a high-energy shelf to be a uniquely Phanerozoic phenomenon without Proterozoic or Archean analogs. The lack of volumetrically significant pre-Ediacaran phosphorites thus more likely reflects limited P enrichment in the early stages of sedimentation than changes in physical oceanography. With sufficiently low P content in surficial sediments, even ideal winnowing conditions or very low sedimentation rates are unlikely to produce large phosphorite-grade P enrichments.

An alternative explanation is that the geochemistry of the pre-Ediacaran oceans was unfavorable for apatite formation, and thus phosphorites were unlikely to form even in settings with rapid P delivery and efficient winnowing. This is an appealing argument given that apatite formation has been linked to bacterial responses to fluctuating redox conditions (40). However, authigenic apatite formation occurs in a wide range of redox conditions in modern environments and the relevant precursors can accumulate within many different types of organisms (41). We therefore consider the rate of P delivery, rather than the existence of favorable tectonic, ecological, or geochemical conditions, the most likely culprit in driving the transition to an age of recurrent phosphogenesis.

What could have happened during the Ediacaran Period to enable the rates of P delivery necessary for modern-style phosphogenesis on continental shelves and platforms? An increase in P delivery could, in principle, reflect the changing composition of eroding continental crust; however, a compilation of elemental compositions for more than 170,000 igneous rocks formed throughout Earth's history shows no particular signature of increasing bulk P associated with the Ediacaran state change in phosphogenesis (42). Ediacaran phosphogenesis does coincide with Pan-African orogenesis (20) and elevated $^{87}Sr/^{86}Sr$ in limestones (43, 44), suggesting high rates of denudation. However, orogenesis alone provides neither the magnitude nor the persistence required to explain Ediacaran state change. Indeed, a new compilation of P abundance in fine-grained clastic sedimentary rocks of Neoproterozoic and early Paleozoic age shows no systematic change in phosphorus content, implying limited long-term change in net supply or burial (Fig. 2). Our analysis extends a previously published phosphorous database (45), adding 1,731 new measurements that more than double the Neoproterozoic and Cambrian–Silurian phosphorous data that can be examined. (For more details and statistical analyses see *SI Appendix*. All data generated and analyzed during this study are included in Dataset S1.) The most extreme enrichments (often used as indicators of P inventory) do change in magnitude through the late Proterozoic and early Phanerozoic interval, but mass flux contributions are more appropriately captured by overall distributions (Fig. 2). The stability of these distributions across the Neoproterozoic and Paleozoic is consistent with the argument that economic-grade phosphorites reflect a small leak from the ocean, not the lion's share of P burial.

Modern phosphogenesis occurs almost exclusively in upwelling zones (25), where deep water sources almost all new nutrients to the photic zone. This, in conjunction with the lack of support for a sustained increase in riverine supply, suggests that the Ediacaran onset of phosphogenesis may be linked to changes in P

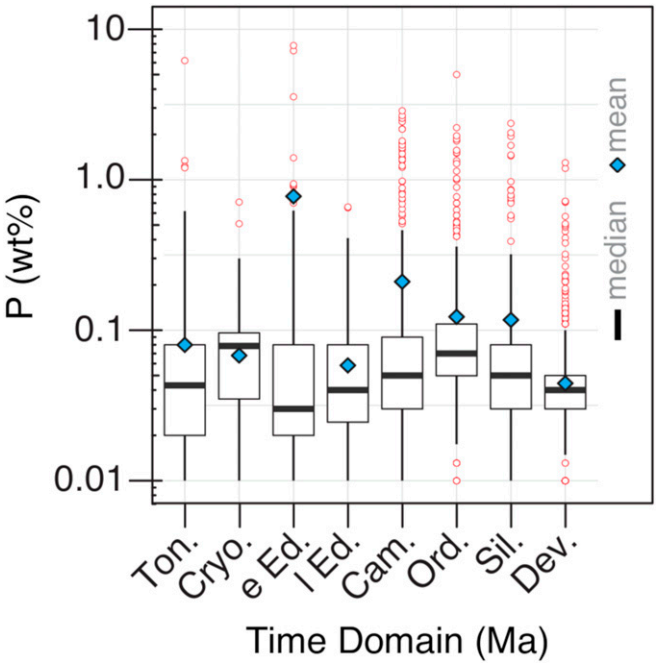

Fig. 2. The phosphorus content of Neoproterozoic and lower Paleozoic sedimentary rocks, including new P measurements as well as published compilations (45). The data are plotted as a box and whisker plot: Center lines indicate medians, boxes the inner quartiles, and whiskers 1.5 times the interquartile range. Outliers falling beyond the whiskers are shown as red dots; these include phosphorites as defined in ref. 25 (wt % P_2O_5 >18%). The mean value is also included for each bin and denoted as a blue diamond. A full analysis of all geological time is available in *SI Appendix*. Pairwise comparison of time bins demonstrates that most time bins are significantly different—not unsurprising given the large number of samples. This gives confidence that the small effect sizes seen are an accurate reflection of the geologic record and not a sampling effect. Dev: Devonian; Sil.: Silurian; Ord.: Ordovician; Cam.: Cambrian; l. Ed.: late Ediacaran; e. Ed.: early Ediacaran; Cryo.: Cryogenian; Ton.: Tonian.

remineralization. In general, an increase in remineralization rate will increase the size of the deep-water P reservoir. Indeed, in modern oceans, the ingrowth of PO_4 in deep water is used as an integrated measure of deep sea oxic respiration. With an eye toward increasing PO_4 liberation in the deep ocean, Ediacaran deep waters would have to either receive more sinking organic matter (electron donors), calling on increased surface ocean primary production, or carry a larger oxidant inventory (electron acceptors), a feature linked to the overall redox state of the ocean–atmosphere system. An Ediacaran increase in the availability of electron acceptors in the deep ocean could have led to increased organic matter remineralization and, hence, an increased regenerative P flux to the surface ocean (46, 47). The resulting increase in productivity and organic matter export could then perpetuate the reorganization of this enhanced phosphorus cycle.

Methods

The effect of remineralization rates on the marine phosphate reservoir can be estimated using a simple mass balance calculation. Phosphorus enters the ocean through continental weathering and is removed by deposition of organic matter to the sediment. There, it can either be buried or remineralized into porewaters, from which it may diffuse to the water column or precipitate in an authigenic phase. Treating the deep ocean as a well-mixed reservoir, a steady-state deep-water phosphorus budget balances regeneration of organic matter derived phosphorus with loss to the photic zone through upwelling (with rate *u*, liters per year). We can define the rate of phosphorus regeneration as the fraction (ε_{regen}) of total organic

phosphorus export to the deep ocean that returns to the dissolved inorganic pool. Given the rate of phosphorus input from weathering (W_P, moles P per year), this yields a simple mass balance expression for the deep-water phosphorus concentration (*SI Appendix*):

$$[P] = \frac{\varepsilon_{\text{regen}}}{1-\varepsilon_{\text{regen}}}\frac{W_P}{u} \quad [1]$$

where

$$\varepsilon_{\text{regen}} \equiv 1 - \frac{r}{\rho}\varepsilon_C. \quad [2]$$

Phosphorus concentrations increase as the regeneration of P becomes more efficient, as measured by $\varepsilon_{\text{regen}}$. This quantity can be expressed in terms of two well-studied parameters, ε_C and ρ. The first, ε_C, is the fraction of organic carbon exported from the photic zone to deep waters that is ultimately buried; ρ is the ratio of organic carbon to total phosphorus in the deep-water sediment. The latter need not be equal to the C:P ratio of organic matter deposited on the seafloor, r—following remineralization, P may be retained in authigenic minerals such as apatite or vivianite, or adsorbed to particle surfaces (48). This result follows directly from mass balance, with $(r/\rho)\varepsilon_C$ defined as the fraction of organic phosphorus export that is ultimately buried in sediments. Note that all information on redox cycling is contained in the two critical geochemical parameters ε_C and ρ. This is a general result for any well-mixed, phosphorus-limited ocean.

Results

The sensitivity of the marine phosphorus reservoir to these processes is shown in Fig. 3. Phosphate concentrations vary by more than a factor of 10 when the range of burial efficiencies and C:P ratios observed in modern anoxic environments is applied to the global ocean. Higher P concentrations occur when a larger fraction of the phosphorus in organic matter is released back to the water column, due to more efficient remineralization (smaller values of ε_C), more efficient return of porewater phosphate to the ocean (smaller r:ρ), or both. A larger reservoir of dissolved phosphate results in more nutrient-rich upwelling, which in turn fuels greater primary production and proportionally higher rates of export, larger oxidant inventories, and ultimately even greater rates of deep-water nutrient regeneration. This cycle provides a positive feedback on changes in the oceanic phosphorus reservoir,

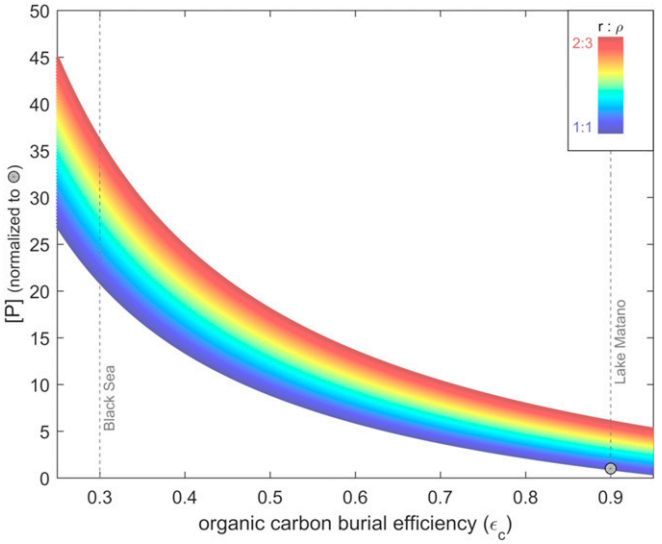

Fig. 3. Deep-sea phosphorus concentration versus the efficiency of organic carbon burial. [P] has been normalized to our estimate for a low-sulfate, ferruginous ocean of the early Neoproterozoic Era. ε_C is the burial efficiency of organic carbon; r is the C:P ratio of organic matter deposited on the seafloor; ρ is the C_{org}:P_{total} ratio in sediments after authigenesis. Calculated values of [P] have been normalized to the result for $\varepsilon_C = 0.9$, $r = \rho$.

resulting in the nonlinear relationships in Fig. 3. Ultimately, this cycle stabilizes when the increase in primary production and export balances the oxygen-mediated drop in burial efficiency, bringing the P cycle back to steady state.

Geochemical data demonstrate that subsurface water masses of the world's oceans remained anoxic until well into the Phanerozoic Eon (33, 49, 50), limiting the direct impact of changing oxygen inventories on deep-water phosphorus remineralization. On the other hand, modeling of sulfur isotopes and evaporite distribution/volume supports the idea that seawater sulfate levels increased in mid-Ediacaran times (34, 35), suggesting that the global influence of sulfate reduction may have increased in tandem with deposition of the earliest major phosphorites. It has been argued that sulfate concentrations in seawater rose from <1 mM to perhaps 6 to 10 mM (51), coincident with maximal Pan-African continental erosion (20, 34, 43). Perhaps more convincing is the observation that extensive sulfate evaporites were deposited in Ediacaran to basal Cambrian basins. Evaporites have precipitated locally to regionally in sedimentary basins throughout recorded geologic time, but the abundance of evaporite minerals has changed dramatically. Volumetric estimates (35) for evaporites deposited over the past 2.5 Ga show that 14 of 34 Ordovician and younger evaporite deposits are larger than 100,000 km^3. In contrast, all of the deposits older than *ca*. 850 Ma are smaller than 30,000 km^3. Larger sulfate-rich evaporites began to form in Australia and northwestern Canada about 810 Ma, perhaps recording transient redox change. Much larger deposits (>100,000 km^3), however, formed only from the late Ediacaran and Cambrian onward. These include evaporitic units that are among the largest ever described—larger than all known Tonian examples combined.

A weathering-mediated increase in sulfate concentration would have enhanced global remineralization of organic matter (i.e., lower values of ε_C). The scale of this change can be estimated by comparing the burial efficiencies of modern anoxic waters masses with different sulfate concentrations. Only 10% of organic matter is remineralized in the anoxic basin of Lake Matano (52) (ε_C ~90%), where sulfate concentrations are <30 μM (53). In contrast, in the anoxic but sulfate-rich Black Sea (15 to 20 mM sulfate concentration), 70% of organic matter is remineralized (ε_C ~30%) (54, 55). Lake Matano and the Black Sea are not perfect analogs for early and late Neoproterozoic oceans, but the sevenfold difference in remineralization rate is consistent with the overall greater availability of terminal electron acceptors in the Black Sea. Following Eq. **1**, this effect alone would have increased the size of the deep water P reservoir in the mid-Ediacaran by a factor of at least 4, if we assume the largest basin-wide ρ values from the modern, or by a factor of 20, given $r \sim \rho$. Smaller values of ρ, which may have been possible if formation of the hydrated iron phosphate mineral vivianite formation was extensive in ferruginous deep waters, would result in even larger factors. We note that even a small increase in dissolved oxygen and aerobic respiration in deeper water masses would further exacerbate the remineralization effect.

In this view, increasing P remineralization accompanies an increase in global sulfate reduction. The global deep-ocean sulfate reduction rate (S) implied by Eq. **1** is given by (*SI Appendix*)

$$S = \frac{1}{2}\frac{(1-\varepsilon_C)}{\varepsilon_C}\rho W_P. \quad [3]$$

For a change from Matano-like (~0.9) to Black Sea–like (ε_C ~0.3) carbon cycling, the sulfate reduction rate is increased 20-fold. However, these conclusions do not necessarily imply a net increase in pyrite burial. Given a modern input of ~100 Gmol reactive $P{\cdot}y^{-1}$ (23) and $\rho \sim r$, the predicted Ediacaran sulfate reduction rate is between roughly 10^{11} and 10^{12} $Tmol{\cdot}y^{-1}$,

distributed over the anoxic oceanic water mass and underlying sediment. This value is several times lower than estimates of modern sulfate reduction rates (56), implying that the Ediacaran sulfur cycle may have been smaller than it is today. Therefore, it is likely that the deep ocean remained ferruginous across this transition, consistent with redox proxy records (33, 49, 50).

Our calculated estimate of a P budget assumes no change in the efficiency with which remineralized porewater phosphorus was returned to the deep-water column; that is, we did not account for potential changes in ρ. Phosphorus retention in sediments is likely governed by precipitation of fluorapatite and, in the ferruginous deep waters of the Proterozoic ocean, ferrous phosphate minerals such as vivianite (57). The latter have been demonstrated to be important P sinks in modern iron-rich porewaters (58). Phosphorus return to the water column is greater in euxinic than in noneuxinic anoxic environments, possibly due to sink competition and the pyritization of vivianite (59). Rising sulfate levels in the Ediacaran oceans would have increased the depth of the sulfate–methane transition zone, increasing the potential for pyritization of vivianite. Thus, by suppressing the ferrous iron sink for phosphorus, rising sulfate levels may have further increased P regeneration and phosphorus upwelling. A significant upturn in the nutrient content of upwelling waters implies a proportional increase in the rate of export production and in the rate of organic carbon delivery to the sediment (11), increasing the potential for phosphorus enrichment in the rock record. This suggests that the onset of major phosphorite deposition was due to the establishment of a large seawater phosphorus reservoir, which encouraged phosphorus burial at sites favorable for subsequent reworking and concentration of apatite; the waxing and waning of these settings with tectonic and oceanographic change led to the episodic nature of Phanerozoic phosphogenesis. Such a change does not require any net increase in the supply or removal of phosphorus from the ocean, consistent with the lack of variation in the median P content of sedimentary rocks (Fig. 2); recall that the molar quantity of P in economic-grade phosphorite deposits is actually quite small when placed against global fluxes. In sum, the mean phosphorus content of fine-grain rocks (Fig. 2) reflects stable erosional input and sedimentary output, while the appearance of phosphorites reflects an increase in the standing pool of marine P as a result of elevated nutrient regeneration and its consequences.

Discussion

We have argued that Ediacaran phosphogenesis was a consequence of rising sulfate concentrations, which enhanced organic P regeneration. The Neoproterozoic increase in marine sulfate evaporite deposition has been hypothesized to reflect a larger sulfate reservoir under elevated pO_2 (60), although the timing and degree of Neoproterozoic oxygenation remains under investigation (33). Major erosional events following the termination of Cryogenian glaciations could also have provided large, if transient, sulfur and phosphorus inputs. Alternatively, erosional fluxes associated with Pan-African orogenesis could account for a later Neoproterozoic increase in marine sulfate levels. Moderate evaporites appear as early as the Tonian, and the $^{87}Sr/^{86}Sr$ ratio in marine carbonates began to increase about 800 Ma (Fig. 1), implying at least some uplift when when the first major sulfate evaporites appeared (44). This was followed by another increase of similar magnitude in the mid-Ediacaran Period, when the first large phosphorites were deposited and marine sulfate levels are thought to have increased markedly (34, 35). Even considering secular increases in $^{87}Sr/^{86}Sr$ associated with mantle evolution, the late Neoproterozoic record shows a striking difference from earlier eras (61). While phosphorus inputs may also have risen during this time, long-term changes in apatite weathering are likely to have been limited by the silicate weathering feedback (62). Sulfur inputs, however, have been exposure-limited since the Paleoproterozoic (63), suggesting that orogenic events could sustain elevated sulfur inputs over longer time scales.

If a pulsed increase in sulfur supply modulates phosphate regeneration, how can we avoid the issue of transience noted earlier? We propose that, due to positive feedbacks, the geochemical changes of the Ediacaran Period were self-sustaining, even if the initial forcing—weathering or otherwise—waned through time. A transient increase in sulfate concentration, deep-ocean sulfate reduction, and phosphorus remineralization leads to additional phosphorus upwelling, permitting phosphorite formation, as discussed above. However, enhanced nutrient upwelling must also drive an increase in net primary production and gross oxygen generation. Surface oxygen concentrations will rise until O_2-sensitive sinks bring the oxygen budget back into equilibrium, consistent with trace-metal redox proxies (19). These sinks include oxic remineralization of organic carbon in shallow water settings, with concomitant nutrient remobilization that promotes further productivity, export, and ultimately a relative shift in carbon burial to anoxic deep waters. The elevated C:P ratios expected in such environments (48) then sustain the initial increase in global O_2 production. A more oxidizing shallow-water environment favors sulfide reoxidation, reinforcing the original increase sulfate concentrations. This positive cycle stabilizes sulfate, oxygen, and phosphorus concentrations at new, higher values.

We explore this behavior using a simple analytical model of the coupled oxygen, sulfur, and phosphorus cycles. Given poor constraints on how global geochemical rates scale with environmental conditions, we consider a minimalist modeling approach the most reasonable test of our conceptual feedback. We parameterize organic carbon and pyrite burial in terms of simple power laws in O_2 and sulfate concentration, respectively (*SI Appendix*). The resulting system can in fact support two stable steady states, with a roughly 10-fold increase in sulfate concentration and a tripling of phosphate concentration (*SI Appendix*, Table S6). Multiple stable states are possible when the oxygen feedback on organic carbon burial efficiency is sufficiently strong. A powerful feedback is required in order to redistribute organic carbon burial to anoxic, P-poor sediments, resulting in cycles of increasing oxygen generation, sulfide reoxidation, and P remineralization. (More precisely, the organic carbon burial efficiency must be more sensitive to changes in pO_2 than the global oxygen sink; *SI Appendix*.) The existence of a strong "oxic effect" on organic burial rates (64) is consistent with this requirement, although firm conclusions await a more precise understanding of the effective global scaling law.

In short, we are argue that the O_2–S–P budget can plausibly be balanced in two different states. The first has relatively low concentrations of surface oxygen, deep-water phosphorus, and marine sulfate. The other has relatively high concentrations of all three species and is characterized by a relative transfer of sulfur burial away from oxidizing surface sediments into deep-water anoxic sediments where the burial efficiency remains high. The onset of bioturbation may also have contributed to sustained increases in $[SO_4^{2-}]$ by irrigating organic-rich surficial sediments (65). It has been argued that both the abundance and depth of animal burrows (described mostly from organic-lean sandstones) were limited in Lower Paleozoic successions (66), but even millimeter-scale irrigation of organic rich muds would influence the global sulfur cycle, a condition already achieved early in the Cambrian Period, if not earlier (67). An increase in marine phosphorus concentrations, upwelling, and organic carbon deposition on continental shelves must have led to an increase in net oxygen production and pO_2. Unsurprisingly, therefore, concentrations of redox-sensitive trace metals suggest an Ediacaran increase in oxygen availability at this time (18, 68). This increase

has been attributed to other positive geochemical feedbacks (45, 47), which may work in concert with the effects described here; the cycling we have described has the advantage that it explicitly includes increased remineralization in anoxic deep waters, consistent with both the phosphorite record and iron speciation data (33).

Interestingly, the interwoven tectonic and environmental events of the Ediacaran Period may have a historical precedent. Shields' (61) normalized curve for Sr isotopes in seawater through time actually shows two prominent peaks, with the Ediacaran rise preceded by a temporally bounded Paleoproterozoic maximum around 2,000 Ma. Thus, the mechanisms we call on to drive end-Proterozoic state shift might also have been in play early in the eon. In fact, Paleoproterozoic rocks not only record a normalized peak in seawater Sr isotopes but also include the first major sulfate-bearing evaporites (69), a cluster of moderately sized phosphorite deposits (2, 70), and evidence for atmospheric oxygen increase (19). It has been argued that Paleoproterozoic oxygen reached levels close to those of the present, but if so this did not persist, perhaps curtailed by high fluxes of hydrothermal fluids into later Proterozoic oceans, recorded by Si isotopes (71) and a resurgence in the deposition of iron formations (72). No comparably strong Sr isotope, phosphorite, or sulfate signatures occur between this interval and the Ediacaran shift, suggesting that tectonics twice facilitated ecosystem change during the Proterozoic Eon.

Returning to the Ediacaran, increasing surface ocean nutrient availability should change the composition of marine phytoplankton as well as rates of photosynthesis. Ecological data and models indicate that cyanobacteria tend to dominate marine phytoplankton when nutrient levels (and so, rates of primary production) are low; as resources increase larger eukaryotic algae tend to take over and dominate (17). Packing biomass and energy into larger eukaryotic phytoplankton will result in more resources being transferred to higher levels in food webs (18), facilitating evolutionary change throughout ecosystems. Biomarker geochemistry suggests that eukaryotic algae first became ecologically prominent in marine phytoplankton only toward the end of the Proterozoic Eon, with marine eukaryotes emerging as permanently and globally important primary producers by 570 to 580 Ma (13, 14). Encouragingly, microfossils and molecular clocks also suggest that green algal clades important in the modern marine phytoplankton radiated in the later Neoproterozoic Era (15, 16). Thus, the late Neoproterozoic rise of eukaryotic phytoplankton provides an indication of increasing nutrient availability and primary production, consistent with an increase in the oceanic phosphorus reservoir suggested here. Consistent with the phytoplankton record, it has been argued that the morphology and development of the earliest known macroscopic animals reflect adaptations for garnering newly available food resources (10). By 560 Ma, motile macroscopic bilaterians, which would have required more food and oxygen than their sessile ancestors (9), also began to diversify. A direct link between marine P concentration and ecosystem structure and size has also recently been found in an Earth system model (73), consistent with our hypothesis linking these ecosystem changes to increased remineralization of organic phosphorus via sulfate reduction.

Conclusions

Even though economic-grade phosphorite deposits account for less than 0.01% of sedimentary P burial, their dramatic expansion during the Ediacaran Period signals a fundamental reorganization of Earth's phosphorus cycle. Importantly, the observed phosphorite expansion is decoupled from the relatively static record of overall P abundance in shales through time; our compilation of phosphate concentrations in Late Neoproterozoic and Paleozoic shales (best recorded by median values rather than means influenced by the extreme enrichments of ore-grade phosphorites) shows little evidence of pronounced secular change. The observed change in phosphorite abundance, then, must reflect increased remineralization of P at depth and its enhanced return to shallow waters via upwelling.

In Proterozoic oceans, phosphorus remineralization and upwelling were limited by oxidant availability in the deep ocean and the sequestration capacity of sediment porewaters. Multiple lines of geochemical evidence indicate that subsurface water masses remained predominantly anoxic well into the Paleozoic Era, so increased Ediacaran oxidant availability was not provided by O_2 per se. Rather, a substantial Ediacaran increase in sulfate evaporites suggests that elevated seawater sulfate concentrations enhanced remineralization by sulfate-reducing bacteria. Enhanced sulfate reduction has important consequences for P burial, but it need not have occurred at rates capable of titrating iron from anoxic water masses. The observed Ediacaran state change was likely initiated by terminal Proterozoic orogenesis, which increased sulfide weathering and erosion in exposed sedimentary rocks. This state change was perpetuated, in turn, by feedbacks in which sulfate-driven increases in P remineralization and upwelling enhanced rates of primary production, further increasing oxidant supply and P remineralization. In short, a state change in phosphorus cycling, initiated by terminal Proterozoic orogenesis and sustained by biospheric feedbacks, precipitated the environmental and biological changes that collectively ushered in the Phanerozoic Eon.

Data Availability. New and compiled geochemical data in Fig. 2 are available in *SI Appendix* and Datasets S1 and S2.

ACKNOWLEDGMENTS. A.H.K. thanks Mick Follows for helpful discussion and the NASA Astrobiology Institute for financial support. E.A.S. thanks the NSF Division of Environmental Biology (Grant 1747731) for support. We thank Emmy Smith and Jessica Creveling for helpful feedback; Emmy Smith, Sam Ritzer, Justin Strauss, Tiffani Fraser, and Francis Macdonald for help collecting samples; and Una Farrell for help compiling phosphorous data.

1. N. J. Planavsky *et al*., A case for low atmospheric oxygen levels during Earth's middle history. *Emerg. Top. Life Sci.* **2**, 149–159 (2018).
2. P. W. Crockford *et al*., Triple oxygen isotope evidence for limited mid-Proterozoic primary productivity. *Nature* **559**, 613–616 (2018).
3. A. H. Knoll, Paleobiological perspectives on early microbial evolution. *Cold Spring Harb. Perspect. Biol.* **7**, a018093 (2015).
4. G. M. Narbonne, J. G. Gehling, Life after snowball: The oldest complex Ediacaran fossils. *Geology* **31**, 27–30 (2003).
5. J. F. Hoyal Cuthill, J. Han, Cambrian petalonamid *Stromatoveris* phylogenetically links Ediacaran biota to later animals. *Palaeontology* **61**, 813–823 (2018).
6. M. A. Fedonkin, "New data on *Kimberella*, the Vendian mollusc-like organism (white sea region, Russia): Palaeoecological and evolutionary implications" in *The Rise and Fall of the Ediacaran Biota*, P. Vickers-Rich, P. Komarower, Eds. (Geological Society of London, 2007), Vol. 286, pp. 157–179.
7. L. A. Buatois, M. G. Mángano, "Ediacaran ecosystems and the dawn of animals" in *The Trace-Fossil Record of Major Evolutionary Events, Topics in Geobiology 39*, M. G. Mángano, L. A. Buatois, Eds. (Springer Verlag, 2016), pp. 27–72.
8. E. Pecoits *et al*., Bilaterian burrows and grazing behavior at >585 million years ago. *Science* **336**, 1693–1696 (2012).
9. E. A. Sperling, A. H. Knoll, P. R. Girguis, The ecological physiology of Earth's second oxygen revolution. *Annu. Rev. Ecol. Evol. Syst.* **46**, 215–235 (2015).
10. J. F. Hoyal Cuthill, S. Conway Morris, Nutrient-dependent growth underpinned the Ediacaran transition to large body size. *Nat. Ecol. Evol.* **1**, 1201–1204 (2017).
11. E. A. Sperling, R. G. Stockey, The temporal and environmental context of early animal evolution: Considering all the ingredients of an "explosion". *Integr. Comp. Biol.* **58**, 605–622 (2018).
12. J. J. Brocks, The transition from a cyanobacterial to algal world and the emergence of animals. *Emerg. Top. Life Sci.* **2**, 181–190 (2018).
13. J. J. Brocks *et al*., The rise of algae in Cryogenian oceans and the emergence of animals. *Nature* **548**, 578–581 (2017).
14. Y. Hoshino *et al*., Cryogenian evolution of stigmasteroid biosynthesis. *Sci. Adv.* **3**, e1700887 (2017).
15. K. R. Arouri, P. F. Greenwood, M. R. Walter, Biological affinities of Neoproterozoic acritarchs from Australia: Microscopic and chemical characterisation. *Org. Geochem.* **31**, 75–89 (2000).

16. P. Sánchez-Baracaldo, J. A. Raven, D. Pisani, A. H. Knoll, Early photosynthetic eukaryotes inhabited low-salinity habitats. *Proc. Natl. Acad. Sci. U.S.A.* **114**, E7737–E7745 (2017).
17. B. A. Ward, S. Dutkiewicz, M. J. Follows, Modelling spatial and temporal patterns in size-structured marine plankton communities: Top-down and bottom-up controls. *J. Plankton Res.* **36**, 31–47 (2014).
18. A. H. Knoll, M. J. Follows, A bottom-up perspective on ecosystem change in Mesozoic oceans. *Proc. R. Soc. B* **283**, 20161755 (2016).
19. T. W. Lyons, C. T. Reinhard, N. J. Planavsky, The rise of oxygen in Earth's early ocean and atmosphere. *Nature* **506**, 307–315 (2014).
20. R. J. Squire, I. H. Campbell, C. M. Allen, C. J. L. Wilson, Did the Transgondwanan Super mountain trigger the explosive radiation of animals on Earth? *Earth Planet. Sci. Lett.* **250**, 116–133 (2006).
21. J. J. Williams, B. J. W. Mills, T. M. Lenton, A tectonically driven Ediacaran oxygenation event. *Nat. Commun.* **10**, 2690 (2019).
22. N. J. Planavsky *et al*., The evolution of the marine phosphate reservoir. *Nature* **467**, 1088–1090 (2010).
23. L. R. Kump, Hypothesized link between Neoproterozoic greening of the land surface and the establishment of an oxygen-rich atmosphere. *Proc. Natl. Acad. Sci. U.S.A.* **111**, 14062–14065 (2014).
24. W. H. Schlesinger, E. S. Bernhardt, *Biogeochemistry: An Analysis of Global Change* (Academic Press, 2013).
25. K. Föllmi, The phosphorus cycle, phosphogenesis and marine phosphate-rich deposits. *Earth Sci. Rev.* **40**, 55–124 (1996).
26. D. Papineau, Global biogeochemical changes at both ends of the proterozoic: Insights from phosphorites. *Astrobiology* **10**, 165–181 (2010).
27. P. J. Cook, J. H. Shergold, Eds., *Phosphate Deposits of the World, Volume 1, Proterozoic and Cambrian Phosphorites* (Cambridge University Press, 1990).
28. G. G. Soares, M. J. Van Kranendonk, E. Belousova, S. Thomson, Phosphogenesis in the immediate aftermath of the great oxidation event: Evidence from the Turee Creek Group, Western Australia. *Precambrian Res.* **320**, 193–212 (2019).
29. C. Zhou *et al*., A new SIMS zircon U-Pb date from the Ediacaran Doushantuo Formation: Age constraint on the Weng'an biota. *Geol. Mag.* **154**, 1193–1201 (2017).
30. H. Cui *et al*., Phosphogenesis associated with the Shuram excursion: Petrographic and geochemical observations from the Ediacaran Doushantuo formation of South China. *Sediment. Geol.* **341**, 134–146 (2016).
31. G. Shields, P. Stille, M. Brasier, "Isotopic records across two phosphorite giant episodes compared: the Precambrian-Cambrian and the late Cretaceous-recent" in *Marine Authigenesis: from Global to Microbial*, C. Glenn, L. Prévôt-Lucas, J. Lucas, Eds. (Society for Sedimentary Geology, 2016), pp. 103–115.
32. T. Tyrell, The relative influences of nitrogen and phosphorus on oceanic primary production. *Nature* **400**, 525–531 (1999).
33. E. A. Sperling *et al*., Statistical analysis of iron geochemical data suggests limited late Proterozoic oxygenation. *Nature* **523**, 451–454 (2015).
34. G. P. Halverson, M. T. Hurtgen, Ediacaran growth of the marine sulfate reservoir. *Earth Planet. Sci. Lett.* **263**, 32–44 (2007).
35. D. A. S. Evans, Proterozoic low orbital obliquity and axial-dipolar geomagnetic field from evaporite palaeolatitudes. *Nature* **444**, 51–55 (2006).
36. A. B. Ronov, V. E. Khain, A. N. Balukhovsky, K. B. Seslavinsky, Quantitative analysis of Phanerozoic sedimentation. *Sediment. Geol.* **25**, 311–325 (1980).
37. C. B. Keller *et al*., Neoproterozoic glacial origin of the great unconformity. *Proc. Natl. Acad. Sci. U.S.A.* **116**, 1136–1145 (2019).
38. M. Cantine, K. Bergmann, A. H. Knoll, Carbonates before skeletons: A database approach. *Earth Sci. Rev.* **201**, 103065 (2020).
39. P. Froelich *et al*., Early diagenesis of organic matter in Peru continental margin sediments: Phosphorite precipitation. *Mar. Geol.* **80**, 309–343 (1988).
40. H. N. Schulz, H. D. Schulz, Large sulfur bacteria and the formation of phosphorite. *Science* **307**, 416–418 (2005).
41. J. Diaz *et al*., Marine polyphosphate: A key player in geologic phosphorus sequestration. *Science* **320**, 652–655 (2008).
42. G. M. Cox, T. W. Lyons, R. N. Mitchell, D. Hasterok, M. Gard, Linking the rise of atmospheric oxygen to growth in the continental phosphorus inventory. *Earth Planet. Sci. Lett.* **489**, 28–36 (2018).
43. Y. Goddéris *et al*., Paleogeographic forcing of the strontium isotopic cycle in the Neoproterozoic. *Gondwana Res.* **42**, 151–162 (2017).
44. Y. Asmerom, S. B. Jacobsen, A. H. Knoll, N. J. Butterfield, K. Swett, Strontium isotopic variations of Neoproterozoic seawater: Implications for crustal evolution. *Geochim. Cosmochim. Acta* **55**, 2883–2894 (1991).
45. C. T. Reinhard *et al*., Evolution of the global phosphorus cycle. *Nature* **541**, 386–389 (2017).
46. M. A. Kipp, E. E. Stüeken, Biomass recycling and Earth's early phosphorus cycle. *Sci. Adv.* **3**, eaao4795 (2017).
47. T. A. Laakso, D. P. Schrag, A small marine biosphere in the Proterozoic. *Geobiology* **17**, 161–171 (2019).
48. T. Algeo, E. Ingall, Sedimentary C_{org}:P ratios, paleocean ventilization, and Phanerozoic atmospheric pO_2. *Palaeogeogr. Palaeoclimatol. Palaeoecol.* **256**, 130–155 (2007).
49. T. W. Dahl *et al*., Devonian rise in atmospheric oxygen correlated to the radiations of terrestrial plants and large predatory fish. *Proc. Natl. Acad. Sci. U.S.A.* **107**, 17911–17915 (2010).
50. W. Lu *et al*., Late inception of a resiliently oxygenated upper ocean. *Science* **361**, 174–177 (2018).
51. C. L. Blättler, K. D. Bergmann, L. C. Kah, I. Gómez-Péreze, J. A. Higgins, Constraints on Meso-to Neoproterozoic seawater from ancient evaporite deposits. *Earth Planet. Sci. Lett.* **532**, 115951 (2020).
52. L. B. Kuntz, T. A. Laakso, D. P. Schrag, S. A. Crowe, Modeling the carbon cycle in Lake Matano. *Geobiology* **13**, 454–461 (2015).
53. S. A. Crowe *et al*., Deep-water anoxygenic photosythesis in a ferruginous chemocline. *Geobiology* **12**, 322–339 (2014).
54. C. Slomp, J. Thomson, G. de Lange, Enhanced regeneration of phosphorus during formation of the most recent eastern Mediterranean sapropel (S1). *Geochim. Cosmochim. Acta* **66**, 1171–1184 (2002).
55. N. Dijkstra *et al*., Phosphorus dynamics in and below the redoxcline in the Black Sea and implications for phosphorus burial. *Geochim. Cosmochim. Acta* **222**, 685–703 (2018).
56. A. R. Waldeck *et al*., Deciphering the atmospheric signal in marine sulfate oxygen isotope composition. *Earth Planet. Sci. Lett.* **522**, 12–19 (2019).
57. L. Derry, Causes and consequences of mid-Proterozoic anoxia. *Geophys. Res. Lett.* **42**, 8538–8546 (2015).
58. T. Jilbert, C. Slomp, Iron and manganese shuttles control the formation of authigenic phosphorus minerals in the euxinic basins of the Black Sea. *Geochim. Cosmochim. Acta* **107**, 155–169 (2013).
59. D. Reed, B. Gustafsson, C. Slomp, Shelf-to-basin iron shuttling enhances vivianite formation in deep Baltic Sea sediments. *Earth Planet. Sci. Lett.* **434**, 241–251 (2016).
60. E. C. Turner, A. Bekker, Thick sulfate evaporite accumulations marking a mid-Neoproterozoic oxygenation event (Ten Stone Formation, Northwest Territories, Canada). *Geol. Soc. Am. Bull.* **128**, 203–222 (2016).
61. G. A. Shields, A normalised seawater strontium isotope curve: possible implications for Neoproterozoic-Cambrian weathering rates and the further oxygenation of the Earth. *eEarth* **2**, 35–42 (2007).
62. J. C. G. Walker, P. B. Hays, J. F. Kasting, A negative feedback mechanism for the long-term stabilization of Earth's surface temperature. *J. Geophys. Res. Oceans* **86**, 9776–9782 (1981).
63. H. D. Holland, *The Chemical Evolution of the Atmosphere and Oceans* (Princeton University Press, 1984).
64. S. Katsev, A. Crowe, Organic carbon burial efficiencies in sediments: The power law of mineralization revisited. *Geology* **43**, 607–610 (2015).
65. D. E. Canfield, J. Farquhar, Animal evolution, bioturbation, and the sulfate concentration of the oceans. *Proc. Natl. Acad. Sci. U.S.A.* **106**, 8123–8127 (2009).
66. L. Tarhan, M. Droser, N. Planavsky, D. Johnston, Protracted development of bioturbation through the early Paleozoic era. *Nat. Geosci.* **8**, 865–869 (2015).
67. R. C. Gougeon, M. G. Mángano, L. A. Buatois, G. M. Narbonne, B. A. Laing, Early Cambrian origin of the shelf sediment mixed layer. *Nat. Commun.* **9**, 1909 (2018).
68. S. K. Sahoo *et al*., Ocean oxygenation in the wake of the Marinoan glaciation. *Nature* **489**, 546–549 (2012).
69. C. L. Blättler *et al*., Two-billion-year-old evaporites capture Earth's great oxidation. *Science* **360**, 320–323 (2018).
70. P. K. Pufahl, "Bioelemental sediments" in *Facies Models*, N. P. James, R. W. Dalrymple, Eds. (Geological Association of Canada, ed. 4, 2010), pp. 477–503.
71. R. Chakrabarti, A. H. Knoll, S. B. Jacobsen, W. W. Fischer, Silicon isotopic variability of Proterozoic cherts. *Geochim. Cosmochim. Acta* **91**, 187–201 (2012).
72. B. Rasmussen *et al*., Deposition of 1.88-billion-year-old iron formations as a consequence of rapid crustal growth. *Nature* **484**, 498–501 (2012).
73. C. T. Reinhard *et al*., The impact of marine nutrient abundance on early eukaryotic ecosystems. *Geobiology* **18**, 139–151 (2020).
74. A. J. G. Notholt, R. P. Sheldon, D. F. Davidson, Eds., *Phosphate Deposits of the World, Volume 2. Phosphate Rock Resources* (Cambridge University Press, Cambridge UK, 1989).